Reliability Assessment of Phased-mission Systems under Random Shocks

Xiang-Yu Li , Yan-Feng Li , Hong-Zhong Huang , Enrico Zio

PII: S0951-8320(17)30539-2
DOI: https://doi.org/10.1016/j.ress.2018.08.002
Reference: RESS 6238

To appear in: *Reliability Engineering and System Safety*

Received date: 6 May 2017
Revised date: 28 July 2018
Accepted date: 1 August 2018

Please cite this article as: Xiang-Yu Li , Yan-Feng Li , Hong-Zhong Huang , Enrico Zio , Reliability Assessment of Phased-mission Systems under Random Shocks, *Reliability Engineering and System Safety* (2018), doi: https://doi.org/10.1016/j.ress.2018.08.002

Highlights

- A reliability model for PMS subject to random shocks is proposed.
- MRGP is used to deal with the dynamic non-exponential components.
- A MC simulation procedure is proposed to evaluate PMS subject to random shocks.
- The result confirms the importance of considering random shocks in PMS reliability.

Reliability Assessment of Phased-mission Systems under Random Shocks

Xiang-Yu Li[1,2], Yan-Feng Li[1,2], Hong-Zhong Huang*,[1,2], Enrico Zio[3,4]

1. School of Mechanical and Electrical Engineering, University of Electronic Science and Technology of China, Chengdu 611731, China
2. Center for System Reliability and Safety, University of Electronic Science and Technology of China, Chengdu 611731, China
3. Chair System Science and the Energy Challenge, Fondation Électricité de France (EDF), CentraleSupélec, Université Paris Saclay, 91192 Gif-sur-Yvette cedex, France
4. Energy Department, Politecnico di Milano, Milano, Italy

ABSTRACT

Phased-mission systems (PMSs) are widely used, especially in the aerospace industry. As in the outer space there are many kinds of cosmic rays, such as the Galactic Cosmic Rays (GCR), randomly hitting on these systems and causing significant impact on the electronics inside or outside the equipment, a reliability model for PMSs considering both finite and infinite random shocks is proposed in this paper. The modularization method is used to simplify the state space model for each

* Corresponding Author: hzhuang@uestc.edu.cn
Tel: +86-28-61831252; Fax: +86-28-61830227.

phase and reduce the amount of system states, and the Markov regenerative process (MRGP) is used to describe the hybrid components' lifetime distributions and the dynamic behaviors within the modules. Then, two kinds of scenarios, finite and infinite random shocks effect, are both integrated into the dynamic modules. For demonstration, a phased altitude and orbit control system (AOCS) subjected to infinite random shocks is illustrated to demonstrate the procedure of the proposed Monte Carlo simulation. Thirdly, the evaluated system reliability under infinite random shocks is compared with the same system without considering random shocks. At last, a sensitivity analysis is also provided for completion.

Keywords: Phased-mission system, random shocks, Markov regenerative process, Monte Carlo simulation, Altitude and Orbit Control System.

NOMENCLATURE

Mi	The ith module after system modularization
M	The states set of the modules
T_n	The phase time of phase n
n	The phase number
u	The arrival rate of the random shocks
λ_S	The failure rate of component S without shocks
λ_S^n	The failure rate of component S after the nth shocks

T_F The recorded module failure time

$R_{sys}(t)$ The system reliability at time t

ACRONYM

AOCS Altitude and orbit control system

BDD Binary decision diagram

CCF Common cause failure

CSP Cold Spare

FDEP Functional DEPendent

FT Fault tree

GCR Galactic Cosmic Ray

MC Monte Carlo

MDD Multi-valued decision diagram

MRGP Markov regenerative process

PMS Phased-mission system

SSE Single Event Effects

1. INTRODUCTION

In this paper, the reliability of phased-mission systems (PMSs) subjected to random shocks is considered. In a PMS, the system needs to perform different tasks in successive time periods, known as phases [1]. A classic example is the manned spacecraft whose missions can be divided into launch, orbit-transfer, on-orbit operation and back-to-earth phases. In these non-overlapping phases, the system

needs to accomplish different mission demands. For these complex and high-value aerospace equipment, reliability is a very critical value. Usually, the reliability of PMSs are defined as the probability that all the consecutive missions are accomplished successfully. The challenges in the reliability assessment of PMSs are mainly due to three aspects: (1) dynamic behaviors within phases, like the CSP (Cold Spare) that is commonly used to improve the system reliability or the FDEP (Functional DEPdenct); (2) dynamic behaviors among phases, whereby the system configuration changes from one phase to another; moreover, in different phases the system will be subjected to different environments, which may lead to different stresses and failure rates [1], [2]; (3) phase dependence, in which the components failed in the former phases will remain failed in the later phases, in non-repairable PMSs [3].

The existing works on the reliability modelling of PMSs can be classified into two major categories:

(1) Combinatorial methods, like Binary Decision Diagram (BDD) [1]-[6] or Multi-valued Decision Diagram (MDD) based models [7]. A BDD is a direct acyclic graph that is based on Shannon decomposition and the graph has two sink nodes, labeled 0 and 1, representing the system working or failure [2]. MDD models are natural extension of traditional BDD models which has multiple outgoing edges to represent the system being in different states [7] that are commonly used in multistate system or system with multiple failure modes. The BDD method was applied by Zang and Trivedi [2] to assess the system reliability of a PMS. Xing applied the BDD

method in the reliability analysis of a generalized PMS, considering the phase-OR as a special case of PMS [3]. Xing also used the BDD method to assess the system reliability of PMS considering common cause failure (CCF) and imperfect coverage [1], and the PMS considering both internal/external CCF [5]. Tang and Dugan assessed the system reliability of PMS considering multimode failures by the BDD method [6]. Besides the BDD modelling, the MDD modelling has also been applied for PMS reliability analysis, especially considering multi-failure modes. Mo [7] pointed out that MDD modelling method is more efficient than BDD in PMS with multi-failure modes. In general, combinatorial methods can assess the system reliability efficiently, especially in large scale systems. But they can only deal with the static system that the primary events in the phase fault tree (FT) model are independent on each other.

(2) State space oriented models, like Markov chain-based or Petri net-based models [8]-[10]. In the state space oriented models, the dynamic behaviors in each phase are represented by state space models, Markov chains or Petri nets. Then the phase dependence is involved in if components' states do not change during the jump of the phases. These models can deal with the dynamic behaviors within phases, like the CSP, but they suffer from the state explosion problem, especially in the large scale system.

To overcome the disadvantages of the methods above, a modularization method combined with combinatorial and state space models is proposed in Refs. [11], [12]. Through the modularization method, the dynamic components are separated as some

into independent modules. As a result, the system can be evaluated by the combinatorial methods and the independent modules. Therefore, the modularization method combines the advantages of both methods.

The PMS considered in this paper is employed in the aerospace industry, e.g. in the manned spacecraft. These systems spend most of their lifetime in the outer space, where they are exposed to many kinds of cosmic rays, such as the Galactic Cosmic Rays (GCRs) [13]. The ionizing nature of GCR particles can pose significant threats to the electronics located onboard, such as the microprocessors to which they may cause memory bit flips and latch-ups. This kind of phenomenon is generally called the Single Event Effect (SSE) [13] and occurs randomly, i.e. as a random shock. If these random shocks are not considered, the reliability of the PMS will be overestimated.

Random shocks have been considered with different approaches in reliability modeling [14]-[24]. Lin and Zio [14] studied the components' reliability considering both degradation processes and random shocks. At the system level, Wang and Pham [17] investigated the influence of the degradation and random shocks, in which the random shocks can lead the system to failure immediately. Rafiee [18] studied cumulative random shocks that increase the components' failure rates. Berker [19] used a semi-Markov model to describe a system under random shocks. Recently, Ruiz-Castro [20] considered the extreme failures and cumulative damage caused by the external shocks. However, these methods are all considered in single-phased systems.

The main contribution of this paper is to integrate random shocks into the reliability modelling of PMSs and a Monte Carlo simulation procedure is then developed for its quantification [26]-[28]. Firstly, the modularization method is used to divide the system into several individual modules so that the complicated system FT model can be simplified. Secondly, the random shocks are integrated into the state space model of the modules by the MRGP. Thirdly, a Monte Carlo method for simulating PMS with random shocks is developed to assess the module reliability. Finally, the reliability of the PMS is evaluated through the PMS-BDD method and the mutually independent modules.

The paper is organized as follows. In section 2, the basic conceptions of the Markov regenerative process and an altitude and orbit control system (AOCS) of the manned spacecraft is introduced in detail. To model the reliability efficiently, the modularization method is applied to simplify its system FT model. Then, the dynamic module is modeled by the MRGP. In section 3, the model for the dynamic module under random shocks is proposed. In section 4, the MC simulation procedure for assessing the reliability of the dynamic module under infinite random shocks is proposed. After that, a dynamic module under finite random shocks is evaluated by the MC simulation and approximation method, respectively, and the reliability comparison result certifies the proposed MC simulation procedure. In section 5, the reliability of the AOCS under infinite random shocks is evaluated by integrating the PMS-BDD method and evaluated module reliabilities in previous. Furthermore, a comparison between the system reliability analysis with and without random shocks is

also provided. Furthermore, the confidence of the MC simulation method and a sensitivity analysis is performed. The modelling procedure is shown in Figure 1. The summary of the work and main conclusions are presented in section 6.

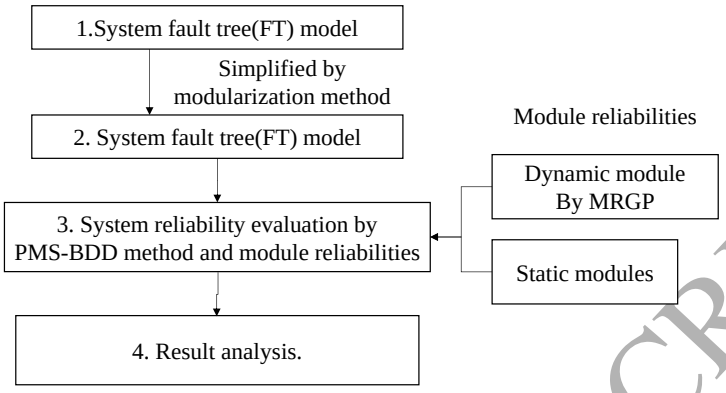

Figure 1. The system reliability evaluation procedure.

2. MRGP AND MULTI-PHASED AOCS

2.1. The Multi-phased AOCS

In this paper, the AOCS of a manned spacecraft under random shocks is studied. The AOCS (altitude and orbit control system) is a critical subsystem of the manned spacecraft to control and adjust its altitude and orbit in the whole lifetime. If the AOCS fails, the manned spacecraft cannot stay in the right altitude and orbit.

A. System Working procedure of AOCS

The AOCS consists of three functional subsystems—the Sensors, the Processors and the Actuators. The working procedure of the AOCS is shown in Figure 2. Firstly, the sensors acquire the altitude and orbit data and send it to the processors. Secondly, the processors process the data and make decisions, and then, the instructions are sent to the actuators. Finally, the actuators adjust the altitude and orbit according to the

instructions. The repetition of this working procedure will keep the spacecraft on the right altitude and orbit during its whole lifetime.

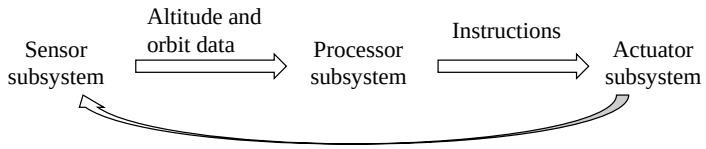

Figure 2. The working procedure of the AOCS

Considering that different missions need to be accomplished at different time, the whole lifetime of the AOCS can be divided into four phases: launching phase, orbital-transfer phase, on-orbit phase and back to earth phase. The phase durations of four phases are $T_1 = 2days$, $T_2 = 4days$, $T_3 = 30days$ and $T_4 = 3days$, which are shown in Figure 3.

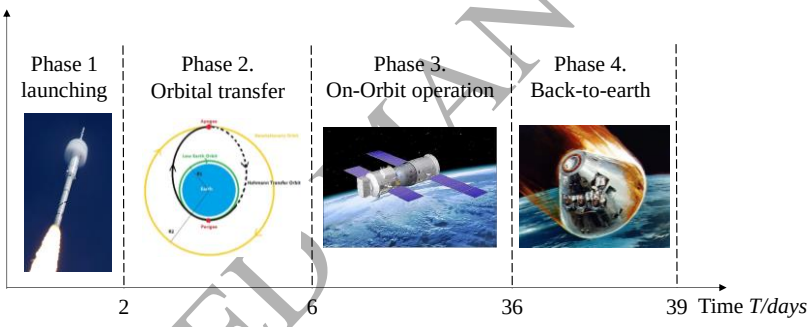

Figure 3. The mission profile for the AOCS.

B. Components and System Structure

As described above, the AOCS is composed of three functional parts;

(1) Micro-computers (Processors): working computer (A), standby computer (B) and a switch component (C). (2) Sensors: Sun sensor (D), Earth sensor (E), Star Track Sensor (F) and Gyro Assembly (G). (3) Actuators: low thrust thrusters (20N, cold standby subsystem, working thruster H, cold standby thruster I and a switch

component S), high thrust thruster (620N, Q), three Momentum wheels (2 out of 3 subsystem, J, K and L).

All the components can be divided into two categories: The working and standby components and the switch components. The lifetime of the complicated working components follow the Weibull distributions ($F(t)=1-e^{-(t/\alpha)^{\beta}}$, where α is the shape parameter and β is the scale parameter). And the lifetime of the switches (electronics) follow the exponential distributions ($F(t)=1-e^{-\lambda t}$, where λ is the failure rate). Due to the confidential requirement, the original data are unavailable, and the parameters of the components are provided by the designers of the spacecraft after being processed, as shown in Tab I.

Tab I. The parameters for the phased AOCS

	A	B	D/E/F/G	H	I	Q	J/K/L
α	1.563	1.725	2.156	2.093	2.185	1.937	1.358
β (days)	138.12	172.65	1291.50	133.15	188.72	332.84	287.47
	C	S					
λ (days)	201.95	216.01					

In the launching phase (1st phase), the spacecraft is launched into the outer space and separated from the rocket. In this phase, the sensors and the processors are necessary to acquire the position data and process it. The processers (A, B and C) and the sensors (D, E, F and G) are necessary. The FT model of phase 1 is shown as Figure 4 (a).

In the orbit-transfer phase (2nd phase), the spacecraft needs to be transferred to the working orbit step by step. Besides the processors and the sensors, the high-thrust thruster 2 and low-thrust thruster 1 are used for the orbit transfer and orbit micro-adjusting, respectively. In this phase, the processers (A, B and C), the sensors (D, E, F and G), the high-thrust thruster (Q) and the low-thrust thruster (H, I and S) are necessary. The FT model of phase 2 is shown as Figure 4 (b).

In the on-orbit phase (3rd phase), the spacecraft works in the normal orbit and the AOCS needs to keep the spacecraft in the correct altitude and orbit. In this phase, except for the micro-computers and sensors, the thruster 1 and momentum wheels are used as actuators to keep the spacecraft working normally on the right orbit. The processers (A, B and C), the sensors (D, E, F and G), the low-thrust thruster (H, I and S) and the movement wheels (J, K and L) are necessary and the FT model of phase 3 is shown as Figure 4 (c).

In the back-to-earth phase (4th phase). The spacecraft need to transfer to the lower orbit and then return to earth. In this phase, the processers (A, B and C), the sensors (D, E, F and G) and the low-thrust thruster (H, I and S) are necessary and the FT model of phase 4 is shown in Figure 4 (d).

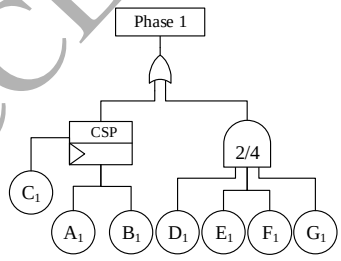

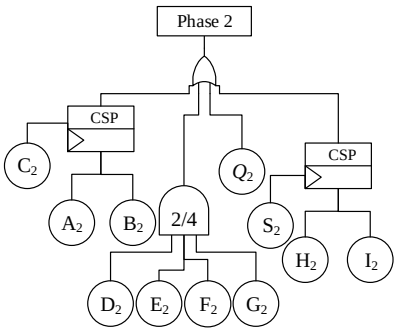

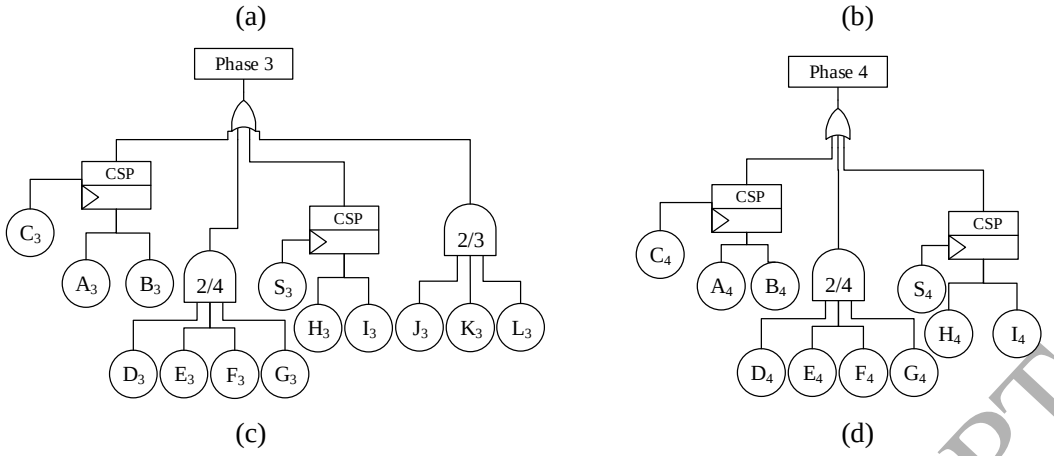

Figure 4. The FT models for each phase of the AOCS

2.2. Simplified by Modularization method

In the previous section, the mission profile and FT models of different phases have been described. Directly applying state-space modeling methods in system modelling for each phase would lead to a very large number of states for each phase, known as the state explosion problem [10], which would make it very difficult to evaluate the system model. In this paper, the modularization method is used to simplify the system FT models and the state explosion problem can be solved to some extent.

The modularization method is proposed by Khoda [29] and used in reliability assessment of PMS by Ou and Dugan [11]. A phase module of a multi-phased system must meet two conditions [11]: (1) each module is a set of the basic events, which means a module must be a subset of all basic events; (2) for each phase, the basic events in the collection should form an independent sub-tree in the modularized fault tree. According to these conditions, all the bottom events in the FT models in Figure 4

of the ACOS can be divided into five independent modules: $M1=(A,B,C)$, $M2=(D,E,F,G)$, $M3=(H,I,S)$, $M4=Q$, $M5=(J,K,L)$, as shown in Figure 5(a)-(e), respectively.

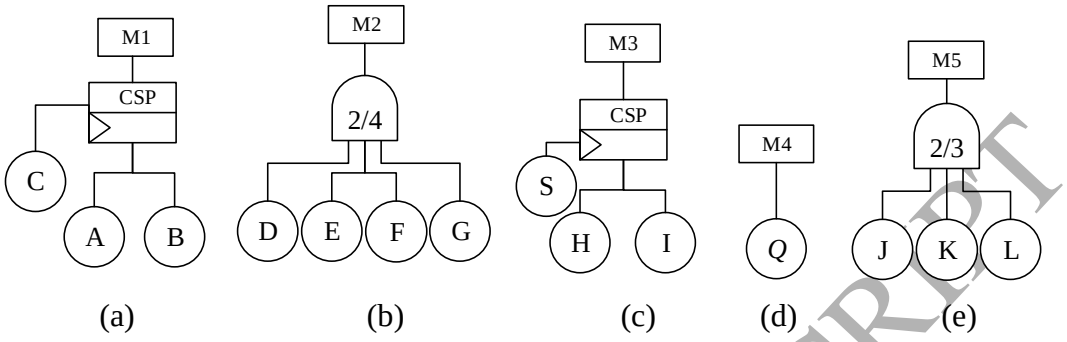

Figure 5. The modules for the AOCS

With these modules, the FT model for the entire multi-phased AOCS after modularization is shown in Figure 6. All the modules can be regarded as independent bottom events in the modularized FT model and the system reliability can be assessed by the PMS-BDD method [2] and the module reliabilities. If there are any dynamic logic gates, the modules are dynamic modules [30]. The reliability of the static modules can be easily evaluated by their own RBD. Moreover, the reliability of the dynamic modules will be evaluated by the Markov regenerative process (MRGP).

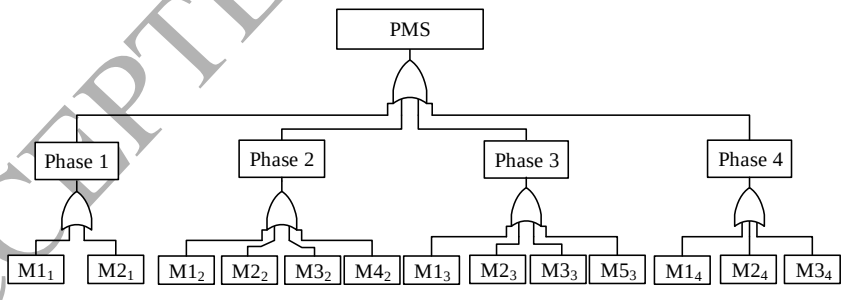

Figure 6. The modularized fault tree of the multi-phased AOCS

2.3. The MRGP model for the dynamic module

A. Basic conceptions of MRGP

In general, a Markov generative process $\{Y(t), t \geq 0\}$ does not possess the Markov property (the memoryless property). But there is a sequence of embedded time sequence within $Y(t)$, the Embedded Markov chain (EMC) $(X, S) = \{X_n, S_n\}$, which is also called the Markov regenerative sequence (MRS). It satisfies the Markov property [25],

$$\begin{aligned} &\Pr\{X_{n+1} = j, S_{n+1} - S_n \leq t \mid X_n = i, \cdots\cdots x_0; S_n, \cdots\cdots, S_0\} \\ &= \Pr\{X_{n+1} = j, S_{n+1} - S_n \leq t \mid X_n = i\} \end{aligned} \tag{1}$$

where X_n and S_n are the state being visited and the *n*th transition time.

S_n in Eq.(1) is the Markov regenerative points and the stochastic process $Y(t)$ possesses the Markov property at these time points. With the embedded MRS (X, S), the MRGP $Y(t)$ satisfies,

$$\Pr\{Y_{t+S_n} = j \mid Y_u, 0 \leq u \leq S_n, X_n = i\} = \Pr(Y_t = j \mid X_0 = i). \tag{2}$$

According to Eq. (2), it can be found that the future of $Y(t)$ from t=S_n only depends on the past only through state X_n. To define a Markov regenerative process, the conditional probability matrix $\boldsymbol{\theta}(t)$ is defined as,

$$\theta_{i,j}(t) = \Pr(Y(t) = j \mid Y(0) = i). \tag{3}$$

In majority of reliability problems involving the MRGP, the primary concern is to evaluate the conditional probability matrix $\boldsymbol{\theta}(t)$. In the evaluation of $\boldsymbol{\theta}(t)$, two

matrices, the $\boldsymbol{Q}(t)$ and $\boldsymbol{E}(t)$, are necessary. $\boldsymbol{Q}(t)=\left[Q_{i,j}(t)\right]$ and $\boldsymbol{E}(t)=\left[E_{i,j}(t)\right]$ are called the global kernel and the local kernel of the MRGP, respectively, which are defined as,

$$\begin{aligned} Q_{i,j}(t) &= \Pr\left\{Y(t)=j, S_1 \le t \mid Y(0)=i\right\} \\ E_{i,j}(t) &= \Pr\left\{Y(t)=j, S_1 > t \mid Y(0)=i\right\} \end{aligned} \tag{4}$$

From Eq. (4), the local kernel, $E_{i,j}(t)$, describes the state transition behavior of the MRGP during two consecutive Markov regenerative epochs $(0, S_1)$ and the global kernel, $Q_{i,j}(t)$, describes the state transition behavior immediately after the next Markov regenerative epoch S_1. With the global kernel $\boldsymbol{Q}(t)$ and the local kernel $\boldsymbol{E}(t)$, the system state transition probability $\boldsymbol{\theta}(t)$ can be evaluated by the Markov renewal equation [25],

$$\boldsymbol{\theta}(t) = \boldsymbol{E}(t) + \int_0^t d\boldsymbol{Q}(t)\boldsymbol{\theta}(t-u). \tag{5}$$

B. Dynamic module evaluation by MRGP

Using the dynamic module M3 is used as an example, the system state evaluation procedure is illustrated as follows:

Step 1: construct the state transition diagram. The state transition diagram of the dynamic module M3 is shown in Figure 7.

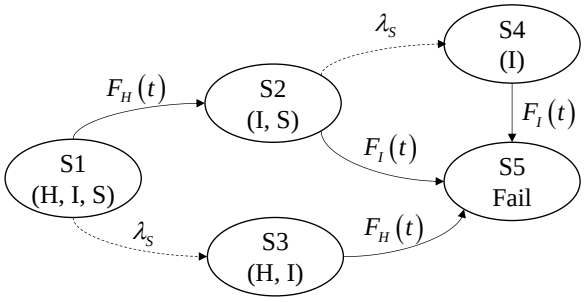

Figure 7. The state transition diagram for module *M*3.

Step 2: identify the structure of the global kernel matrix $\boldsymbol{Q}_{M3}(t)$ and the local kernel matrix $\boldsymbol{E}_{M3}(t)$. According to Figure 7, the exponential transition from state S1 to S3 and from state S2 to S4 are concurrent. It is because that the failure of component S does not affect the failure process of component H and I. So states S3 and S4 are not the Markov regenerative epoch. Hence, this stochastic process shown in Figure 7 is a MRGP whose EMC is identified by states S1, S2 and S5. Accordingly, the global kernel matrix $\boldsymbol{Q}_{M3}(t)$ and the local kernel matrix $\boldsymbol{E}_{M3}(t)$ of this MRGP is,

$$\boldsymbol{Q}_{M3}(t)=\begin{bmatrix} 0 & Q_{1,2}^{M3}(t) & 0 & 0 & Q_{1,5}^{M3}(t) \\ 0 & 0 & 0 & 0 & Q_{2,5}^{M3}(t) \\ 0 & 0 & 0 & 0 & 0 \\ 0 & 0 & 0 & 0 & 0 \\ 0 & 0 & 0 & 0 & 0 \end{bmatrix} \tag{5}$$

$$\boldsymbol{E}_{M3}(t)=\begin{bmatrix} E_{1,1}^{M3}(t) & 0 & E_{1,3}^{M3}(t) & 0 & 0 \\ 0 & E_{2,2}^{M3}(t) & 0 & E_{2,4}^{M3}(t) & 0 \\ 0 & 0 & 0 & 0 & 0 \\ 0 & 0 & 0 & 0 & 0 \\ 0 & 0 & 0 & 0 & E_{5,5}^{M3}(t) \end{bmatrix} \tag{6}$$

Step 3: evaluate all the elements in $\boldsymbol{Q}_{M3}(t)$ and $\boldsymbol{E}_{M3}(t)$. The elements in $\boldsymbol{Q}_{M3}(t)$ and $\boldsymbol{E}_{M3}(t)$ can be computed according to the competing failure mechanism. For example, let T_H , T_I and T_S represent the time to failure of components *H*, *I* and *S*, respectively. Then,

$$\begin{aligned} Q_{1,2}^{M3}(t) &= \Pr\{Y(S_1)=2, S_1 \le t \mid Y(0)=1\} \\ &= \Pr\{\text{'}Componet\ H\ \ fails\ befroe\ component\ S\ \ fails\text{'}\} \\ &= \Pr\{T_H \le t \,\&\, T_S > T_H\} = \int_0^t \Pr\{T_S > u\}\, dF_H(u) = \int_0^t f_H(u)\left(1-F_S(u)\right) du \end{aligned} \tag{7}$$

It should be noted that during the calculation of $Q_{1,2}^{M3}(t)$, the failure of the component *S* does not have any effect on the component I. $Q_{2,5}^{M3}(t)$ can be evaluated as,

$$\begin{aligned} Q_{2,5}^{M3}(t) &= \Pr\left\{\begin{matrix}\text{'}Componet\ I\ \ fails\ befroe\ component\ S\ \ fails\text{'} \\ \text{or '}Componet\ I\ \ fails\ after\ component\ S\ \ fails\text{'}\end{matrix}\right\} \\ &= \Pr\{T_I \le t \,\&\, T_S > T_I\} + \Pr\{T_I \le t \,\&\, T_S \le T_I\} = \Pr\{T_I \le t\} = F_I(t) \end{aligned} \tag{8}$$

Other elements in the global kernel $\boldsymbol{Q}_{M3}(t)$ and the local kernel $\boldsymbol{Q}_{M3}(t)$ can be evaluated in the same way.

Step 4: using the evaluated $\boldsymbol{Q}_{M3}(t)$ and $\boldsymbol{E}_{M3}(t)$, the system state transition probability matrix $\boldsymbol{\theta}_{M3}(t)$ can be evaluated by the Markov renewal equation shown in Eq. (5).

3. INTEGRATING OF RANDOM SHOCKS INTO THE PMS RELIABILTIY MODEL

In this section, the random shocks (e.g. coming from cosmic rays) are integrated into the PMS reliability model. After modularization as described in the last section, all the bottom events in the FT models have been divided into several independent modules. The dynamic module, cold standby module $M3$, is used to describe the model considering random shocks. In module $M3$, H and I are working components and S is the switch component. According to the module description, the state transition diagram of $M3$ is shown in Figure 7. State $S1$ is the perfect working state and $S5$ is the failure state.

As described in the section of Introduction, the randomly coming cosmic rays affect the electronics as random shocks. To integrate the random shocks in the PMS reliability model, some preliminary assumptions are made:

- The arrivals of the random shocks follow a homogeneous Poisson process [14], with a constant arrival rate u (shown in Figure 8). By the opinion of the spacecraft designers, the random shocks occurrence rate is set to be 5 days once and u=1/5$days^{-1}$ in this paper.
- The random shocks are s-independent of the components' failure process.
- The damage brought by the random shocks is cumulative, and in particular, the random shocks increase the failure rate of a constant amount ε at each time they occur and cannot lead the components to failure directly.

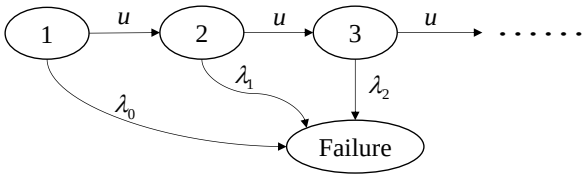

Figure 8. The infinite random shocks process

In this paper, we assume that M indicates the system state and N indicates the number of random shocks that have occurred. To integrate the random shocks in the PMS reliability model, the system state indicator is extended from M into (M,N). After integrating the random shocks as shown in Figure 8 into the state transition diagram of Figure 7, the state transition diagram with random shocks for module $M3$ is shown in Figure 9.

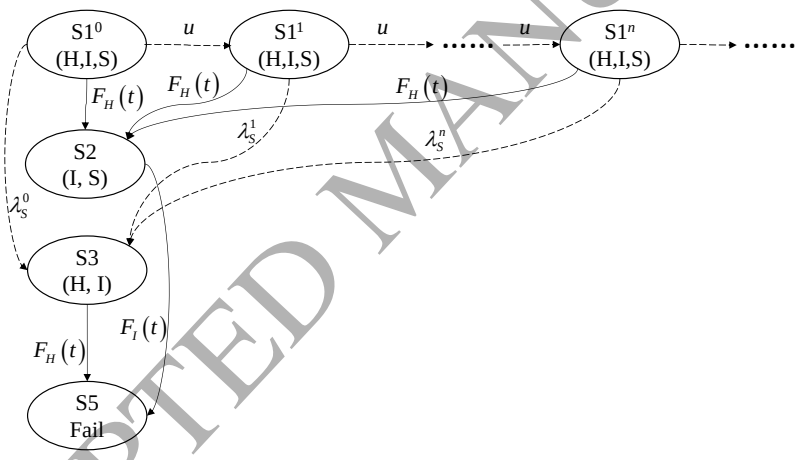

Figure 9. The state transition diagram under random shocks for module *M*3

Furthermore, the failure rates after n random shocks λ_S^n in Figure 9 are set to $\lambda_S^n=\lambda_S(1+\varepsilon)^n$ [14], where λ_S represents the transition rate of the system from state i to state j without random shocks and $(1+\varepsilon)^n$ characterizes the cumulative effect of

the random shocks. By the opinion of experts, the failure rate increment ε, due to a shock, is set to be 0.3 in the case study of this paper. Due to the infinite state number of dynamic module under infinite random shocks, the Monte Carlo (MC) simulation method [26], [27] is applied to assess the PMS reliability in this paper. The MC simulation for evaluating the PMS reliability under random shocks.

3.1. The simulation procedure for dynamic modules

The MC simulation method for the reliability assessment is based on repeated sampling of realizations of system state configurations and computation of the system failure frequency [31], [32]. In this paper, the simulation procedure is conducted to evaluate the reliability of the dynamic module. During each simulation, two quantities, i.e. the number of random shocks N and the module failure time T_F, are recorded. In each repeated simulation, the failure time of the dynamic module, T_{F,M_i}, is simulated y the sampled components' failure time and the logic within the dynamic module. Using the module M3 as an example, the simulation procedure for the dynamic modules is shown in Figure 10.

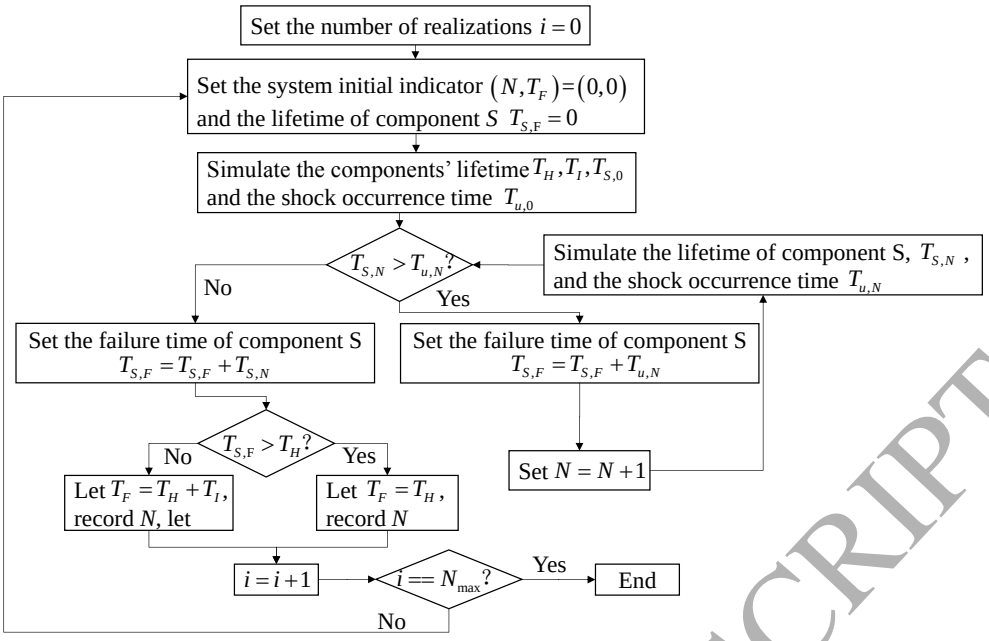

Figure 10. The simulation procedure for dynamic module under infinite shocks.

3.2. Certification of the MC simulation

In this section, to certify the proposed MC simulation procedure, the reliability of module M3 under finite random shocks by the proposed MC simulation method is compared to the reliability of the same system by the MRGP and computed by an approximation method.

Considering a scenario that each random shock on component *S* in module 3 does not only lead to the increasing of its failure rate, it also has the cumulative shock damage and the component will fail after a certain number of random shocks because the cumulative damage reaches the failure threshold [17], [31]. If component *S* fails after the 3rd shocks occur, the state transition diagrams for component *S* under finite random shocks and module 3 under finite random shocks are shown in Figure 11 and Figure 12, respectively.

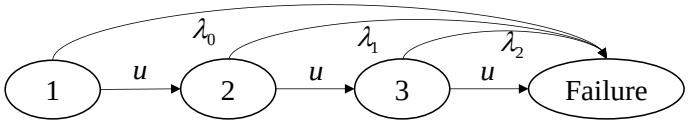

Figure 11. The state transition diagram for component S under finite shocks.

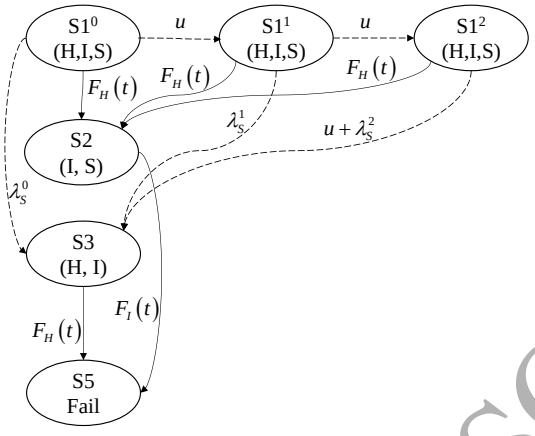

Figure 12. The state transition diagram for *M*3 under finite shocks.

According to the system description in section 2.3, the unreliability of module *M*3 at time *t* is the system state transition probability $\theta_{1,5}^{M3}(t)$. By the Markov renewal equation shown in Eq. (5), the state transition probability $\theta_{1,5}^{M3}(t)$ can be evaluated as,

$$\theta_{1,5}^{M3}(t)=\int_0^t q_{1,5}^{M3}(u)\theta_{5,5}^{M3}(t-u)\,du+\int_0^t q_{1,2}^{M3}(u)\theta_{2,5}^{M3}(t-u)\,du \tag{9}$$

where $q_{i,j}^{M3}(t)=dQ_{i,j}^{M3}(t)/dt$.

In Eq. (9), $\theta_{5,5}^{M3}(t)$=1 and $\theta_{2,5}^{M3}(t)$=$F_I(t)$. Then, the $q_{1,5}^{M3}(t)$ and $q_{1,2}^{M3}(t)$ can be computed as,

$$\begin{aligned} q_{1,5}^{M3}(t)&=F_S(t)\,dF_H(t)\\ q_{1,2}^{M3}(t)&=\left(1-F_S(t)\right)dF_H(t)\end{aligned} \tag{10}$$

where $F_H(t)$ is the CDF of component H ($F_H(t)=1-\exp\left(-\left(t/\alpha_H\right)^{\beta_H}\right)$). $F_S(t)$ is the CDF of component *S* under finite random shocks and it can be evaluated by the CTMC [10],

$$F_S(t)=1-\frac{\left(u\left(\lambda_2-\lambda_S+u\right)+\lambda_2\left(\lambda_1-\lambda_S\right)+\lambda_S^2\right)}{\left(\lambda_S-\lambda_1\right)\left(\lambda_S-\lambda_2\right)}\exp\left(-\left(\lambda_S+u\right)t\right)$$
$$-\frac{u^2}{\left(\lambda_S-\lambda_2\right)\left(\lambda_1-\lambda_2\right)}\exp\left(-\left(\lambda_2+u\right)t\right)-\frac{\left(\lambda_2u-\lambda_1u+u^2\right)}{\left(\lambda_S-\lambda_1\right)\left(\lambda_1-\lambda_2\right)}\exp\left(-\left(\lambda_1+u\right)t\right) \tag{11}$$

where u is the arriving rate of the random shocks and λ_i is the failure rate of component *S* after the *i*th shocks $\lambda_i=\lambda_S\left(1+\varepsilon\right)^i$.

To compute the complicated integrals in Eq. (9), an accurate approximation method, the trapezoidal integration method [33], [34], is applied in this paper and shown as,

$$\int_0^t q_{i,k}(\tau)\theta_{k,j}(t-\tau)d\tau\approx\frac{1}{2}\sum_{i=1}^{n}\left[q_{i,k}(\tau_i)\theta_{k,j}(t-\tau_t)\right]\left[q_{i,k}(\tau_{i+1})\theta_{k,j}(t-\tau_{i+1})\right] \tag{12}$$

where the integration interval $[0,t]$ is divided into *n* equal segments, so the length of each segment is $\delta=t/n$. Integrating Eqs. (10)- (12) into Eq. (9), the system state transition probability $\theta_{1,5}^{M3}(t)$ can be evaluated. Then, the comparison between the reliabilities of module *M*3 by the proposed MC simulation procedure and the MRGP as well as the approximation method is shown in Figure 13.

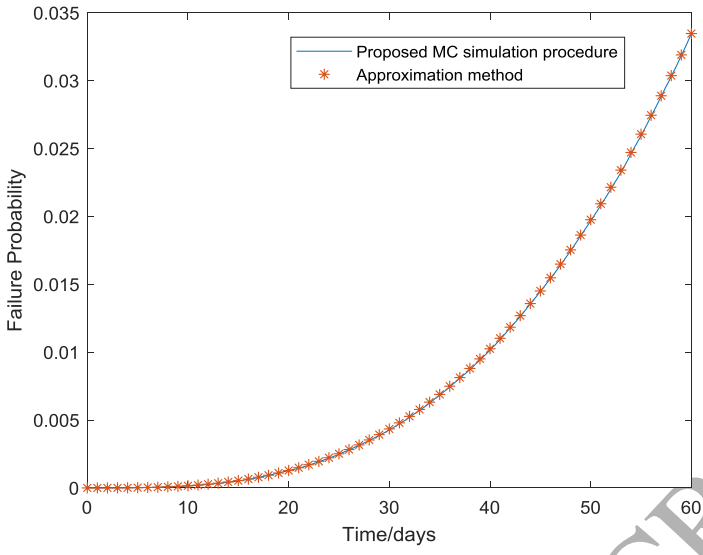

Figure 13. The comparison of module M3 under finite random shocks by different methods.

The results in Figure 13 demonstrate that the proposed MC simulation procedure for the module under random shocks can provide a relatively accurate result.

4. RELIABILITY ASSESSMENT ANALYSIS

4.1. System reliability assessment by PMS-BDD model

In section 2.2, the complex FT model of the AOCS is simplified as the modularized FT model and all the bottom events of the modularized FT are independent on each other. Then, the system reliability can be evaluated by the widely used PMS-BDD model. Considering the phase dependence by the phase algebra proposed in Ref. [6], the system reliability of the phased AOCS can be evaluated by the PMS-BDD model by several steps that are described as follows:

Step 1: transit the FT model of each phase into the corresponding BDD model of each phase. The BDD models for the four phases of the AOCS are shown in Figure 14.

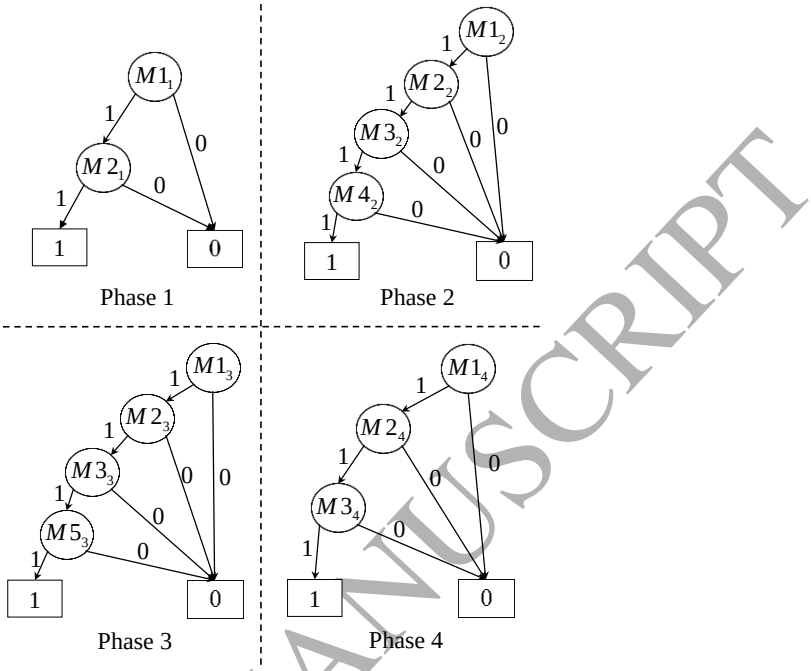

Figure 14. The modularized BDD model for each phase of the AOCS.

Step 2: integrate the BDD models for phases into the system BDD models by the PMS-BDD method. There are two kind of sort orders in the PMS-BDD, the backward PDO and the forward PDO. And through the backward PDO, the system BDD model is much smaller. By the backward PDO and taking the order $M1_4 < M1_3 < M1_2 < M1_1 < M2_4 < M2_3 < M2_2 < M2_1 < M3_4 < M3_3 < M3_2 < M4_2 < M5_3$. Then, the system BDD models in the first two phases, in first three phases and in all four phases is shown in Figure 15(a), (b), and (c), respectively.

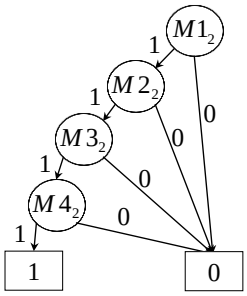

(a). First two Phase

(a) System BDD model for the first two phases.

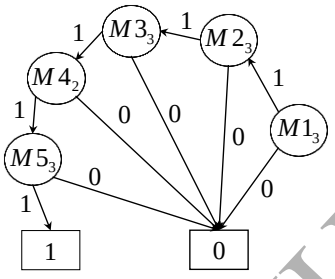

(b) System BDD model for the first three phases.

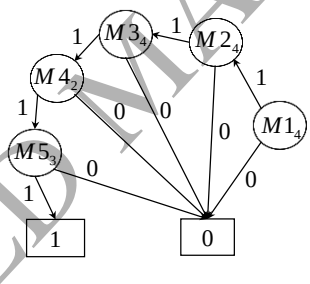

(c) System BDD model for the all the four phases.

Figure 15. The system BDD models for different phases.

Step 3: according to the system BDD models shown in Figure 15, we can get the disjoint paths for the ACOS in phase 1 (η_1), in the first two phases(η_2), in the first three phases(η_3) and in all four phases are(η_4),

$$\begin{cases} \eta_1 = M1_1 M2_1 \\ \eta_2 = M1_2 M2_2 M3_2 M4_2 \\ \eta_3 = M1_3 M2_3 M3_3 M4_2 M5_3 \\ \eta_4 = M1_4 M2_4 M3_4 M4_2 M5_3 \end{cases} \tag{13}$$

Step 4: integrate all the reliability indices of the module reliabilities and include the dynamic and static modules. As a result, the system reliability in different phases can be evaluated as,

$$R(t) = \begin{cases} R_{M1}(t) R_{M2}(t), & 0 < t \le T_1 \\ R_{M1}(t) R_{M2}(t) R_{M3}(t - T1) R_{M4}(t - T1), & T_1 < t \le T_1 + T_2 \\ R_{M1}(t) R_{M2}(t) R_{M3}(t - T1) R_{M5}(t - (T1 + T2)) R_{M4}(T2), & T_1 + T_2 < t \le T - T_4 \\ R_{M1}(t) R_{M2}(t) R_{M3}(t - T1) R_{M5}(T3) R_{M4}(T2), & T - T_4 < t \le T \end{cases} \tag{12}$$

where $T = \sum_{i=1}^{4} T_i$.

4.2. Results

A.Comparison with the system without shocks

The MC simulation of the system mission profile was performed with 2×10^5 histories in this paper. The system reliability of the phased AOCS considering random shocks is represented as the dashed line in Figure 16. Moreover, the reliability of the same system without random shocks is represented as the solid line in Figure 16. The reliabilities of the AOCS at the end of each phase are also shown in Tab II, as well as the relative difference between the reliabilities with and without random shocks and the average numbers of shocks in each phase.

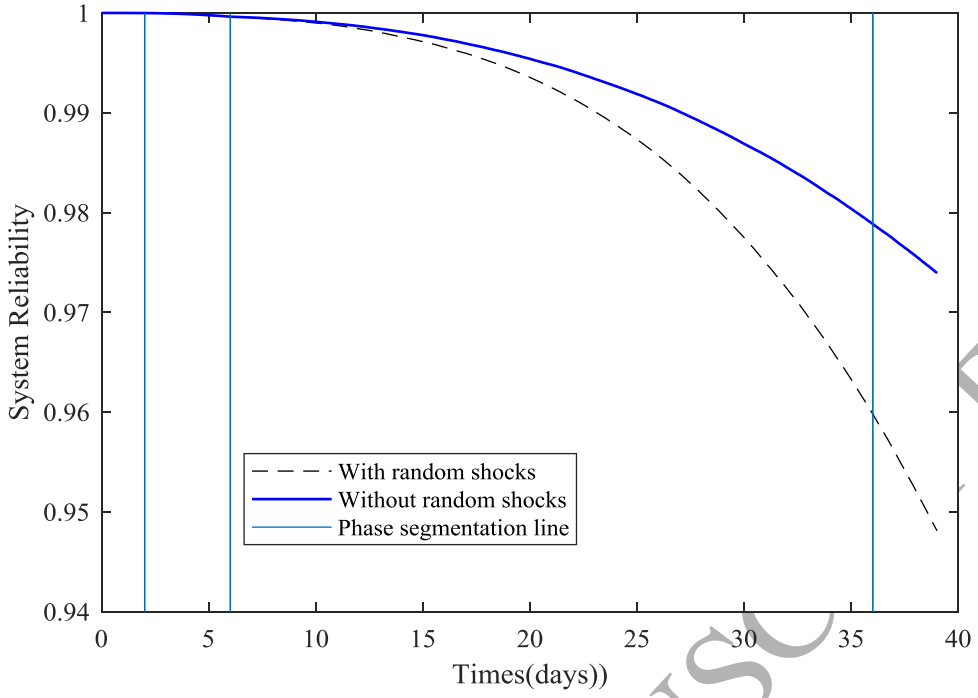

Figure 16. The reliability of the AOCS with and without random shocks

Tab II. The results for the AOCS with and without random shocks

	Phase 1	Phase 2	Phase 3	Phase 4
$R_{sys}^{noshock}(t)$	0.999990	0.999624	0.97885	0.973937
$R_{sys}^{shocks}(t)$	0.999988	0.999613	0.95980	0.948101
Relative difference	1.5000-06	1.1002e-05	0.0198	0.0272

As expected, when the AOCS travels a long time in the outer space, the system reliability is lower than that when considering random shocks, especially in phase 3 and phase 4. If the random shocks are not considered in the modeling, the system reliability may be overestimated.

B.Model confidence

In this section, following the proposed MC simulation procedure, the reliability of the AOCS under infinite shocks and without shocks are evaluated. To assess the confidence of the estimated AOCS reliability under infinite random shocks, the system reliability evaluation by the MC simulation procedure are repeated for $N = 200$ times and the results are shown in Tab III.

Tab III. The reliabilities for the AOCS under random shocks

Time (days)	0	0.1	0.2	……	39
$R_{sys,1}^{shocks}$	1	1.000	1.000	……	0.9429
$R_{sys,2}^{shocks}$	1	1.000	1.000	……	0.9431
……	……	……	……	……	……
$R_{sys,N=200}^{shocks}$	1	1.000	1.000	……	0.9426

With the system reliabilities at different time shown in Tab III, the mean reliabilities values at different times are shown as the solid line in Figure 17. The upper and lower bounds of the 95% confidence of the reliability values at different times are represented as dashed lines in Figure 17, respectively. Consequently, it can be concluded that the proposed MC simulation method can provide accurate results with 2×10^5 realizations.

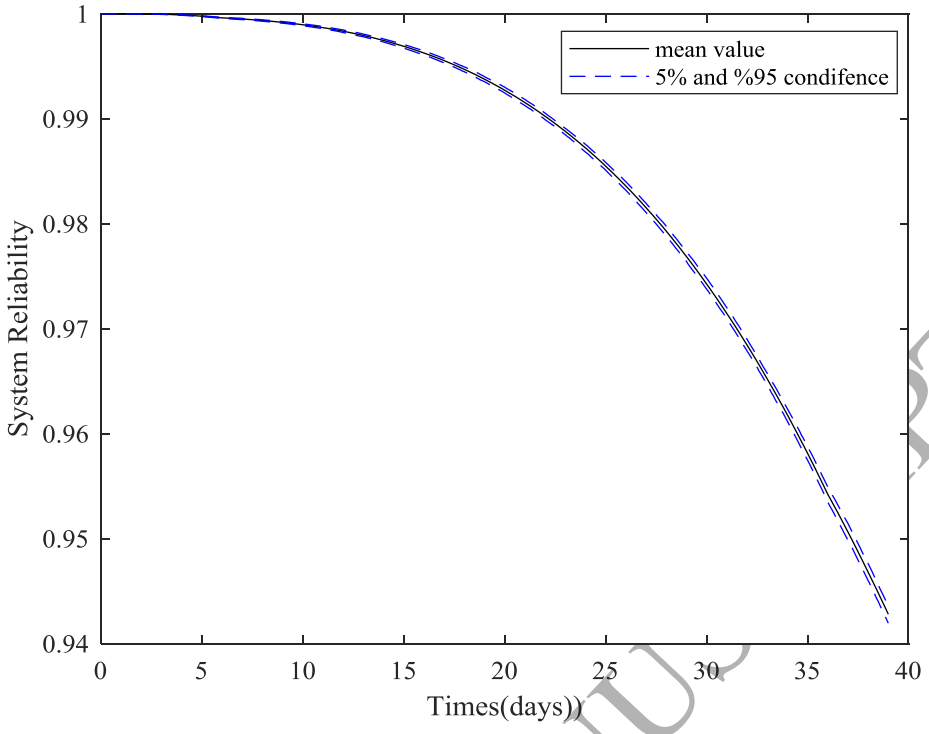

Figure 17. The upper and lower bounds of the 95% confidence of the proposed MC method with 2×10^5 realizations.

4.3. Sensitivity Analysis

In this paper, the effect of random shocks to the PMS is studied. With respect to the random shocks modelling, we have analyzed the sensitivity of the system reliability estimates to two parameters which are related to the random shocks effect, the random shocks occurrence rate $u=[1/4,1/6]days^{-1}$ and the relative increment in the transition rates $\varepsilon=[0.2,0.4]$. The estimated system reliabilities for different combinations of the two parameters are shown in Figure 18.

According to the results in Figure 18, it can be seen that with the increase of the relative increment ε or the random shocks occurrence rate u, the system reliability decreases as expected. Higher ε leads to larger components' failure rates, and larger occurrence rate u values result in more random shocks over the whole lifetime, which decreases the system reliability. In Tab IV, the system reliability with parameters ε=0.2 and $u = 1/4 days^{-1}$ is set to the standard and other elements are differences with different parameters combination. As shown in Tab IV, when the same percentage of variation applies to two parameters, ε is more influential than u on the system reliability.

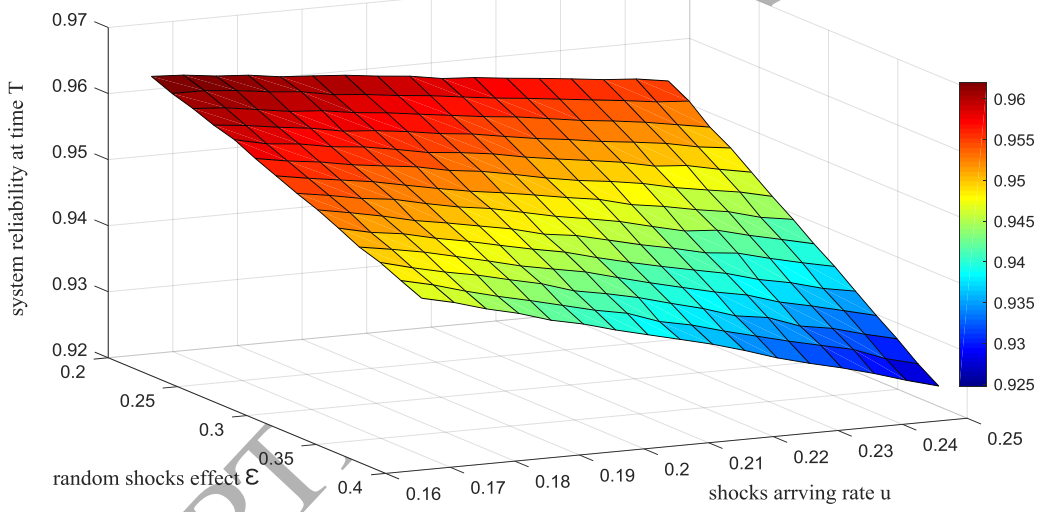

Figure 18. The reliability of the Phased AOCS with and without random shocks for different combinations of u and ε

Tab IV. The errors of the results for the AOCS sensitivity analysis

System reliability error	0.2	0.23	0.26	0.29	0.32	0.35	0.4
0. 247	0%	0.45%	0.98%	1.46%	1.93%	2.42%	3.05%
0.227	0.45%	0.84%	1.31%	1.82%	2.21%	2.65%	3.23%

0.212	0.87%	1.27%	1.66%	2.10%	2.55%	2.85%	3.39%
0.197	1.27%	1.65%	2.03%	2.38%	2.81%	3.07%	3.55%
0.182	1.65%	2.02%	2.35%	2.66%	3.04%	3.25%	3.68%
0.167	2.19%	2.48%	2.74%	3.01%	3.28%	3.52%	3.87%

5. CONCLUSIONS

In this paper, an original reliability model of a PMS subjected to random shocks has been proposed together with a MC simulation procedure for its assessment. Dynamic behaviors, like the cold standby, and different lifetime distributions due to different component types are considered during the modeling.

A practical engineering case, the AOCS in the spacecraft, is used as a case study. To evaluate the system reliability under infinite random shocks effect, a Monte Carlo simulation procedure is proposed. The proposed MC simulation procedure is certified by a dynamic module under finite random shocks. The comparison of the reliability of the system considering the random shocks effect or not confirms the importance of the random shocks effects on the system reliability. At last, the sensitivity analysis involving the parameters that affect the random shocks effect is also carried out to characterize the influences of the random shocks model parameters.

In this paper, only the constant components' lifetime parameters provided by the designers are used to evaluate the reliability of PMS under random shocks. However in reality, the uncertainties of these parameters have significant effects on the robustness of the system model as well as the system reliability, so this will be part of our future work. On the other hand, the shocks arriving rate may not always follow

the homogeneous Poisson process: how to model and assess the system reliability under different random shocks arriving rate process will be another topic of our future research.

ACKNOWLEDGMENTS

This study was sponsored by the National Natural Science Foundation of China under Grant No. 51775090 and China Scholarship Council No.201606070066.

REFERENCES

[1] Xing L. Reliability evaluation of phased-mission systems with imperfect fault coverage and common-cause failures. *IEEE Transactions on Reliability*, 2007, 56(1): 58-68.

[2] Zang X, Sun N, Trivedi K S. A BDD-based algorithm for reliability analysis of phased-mission systems. *IEEE Transactions on Reliability*, 1999, 48(1): 50-60.

[3] Xing L, Dugan J B. Analysis of generalized phased-mission system reliability, performance, and sensitivity. *IEEE Transactions on Reliability*, 2002, 51(2): 199-211.

[4] Levitin G, Xing L, Amari S V. Recursive algorithm for reliability evaluation of non-repairable phased mission systems with binary elements. *IEEE Transactions on Reliability*, 2012, 61(2): 533-542.

[5] Xing L, Levitin G. BDD-based reliability evaluation of phased-mission systems with internal/external common-cause failures. *Reliability Engineering & System Safety*, 2013, 112: 145-153.

[6] Tang Z, Dugan J B. BDD-based reliability analysis of phased-mission systems with multimode failures. *IEEE Transactions on Reliability*, 2006, 55(2): 350-360.

[7] Mo Y, Xing L, Dugan J B. MDD-based method for efficient analysis on phased-mission systems with multimode failures. *IEEE Transactions on Systems, Man, and Cybernetics: Systems*, 2014, 44(6): 757-769.

[8] Alam M, Al-Saggaf U M. Quantitative reliability evaluation of repairable phased-mission systems using Markov approach. *IEEE Transactions on Reliability*, 1986, 35(5): 498-503.

[9] Mura I, Bondavalli A. Markov regenerative stochastic Petri nets to model and evaluate phased mission systems dependability. *IEEE Transactions on Computers*, 2001, 50(12): 1337-1351.

[10] Wang C, Xing L, Levitin G. Competing failure analysis in phased-mission systems with functional dependence in one of phases. *Reliability Engineering & System Safety*, 2012, 108: 90-99.

[11] Ou Y, Dugan J B. Modular solution of dynamic multi-phase systems. *IEEE Transactions on Reliability*, 2004, 53(4): 499-508.

[12] Meshkat L, Xing L, Donohue S K, et al. An overview of the phase-modular fault tree approach to phased mission system analysis *In Proceedings of the International Conference on Space Mission Challenges for Information Technology*, Pasadena, USA, 2003.

[13] Golge S., O'Neill P.M., Slaba T.C. NASA Galactic Cosmic Radiation Environment Model: Badhwar-O'Neill (2014). *34th International Cosmic Ray Conference*, The Hague, Netherlands, 2015.

[14] Lin Y H, Li Y F, Zio E. Integrating random shocks into multi-state physics models of degradation processes for component reliability assessment. *IEEE Transactions on Reliability*, 2015, 64(1): 154-166.

[15] Zheng B, Huang H Z, Guo W, et al. Fault diagnosis method based on supervised particle swarm optimization classification algorithm. *Intelligent Data Analysis*, 2018, 22(1): 191-210.

[16] Mi J, Li Y F, Yang Y J, Peng W, Huang H Z. Reliability assessment of complex electromechanical systems under epistemic uncertainty. *Reliability Engineering & System Safety*, 2016, 152: 1-15.

[17] Li W, Pham H. Reliability modeling of multi-state degraded systems with multi-competing failures and random shocks. *IEEE Transactions on Reliability*, 2005, 54(2): 297-303.

[18] Rafiee K, Feng Q, Coit D W. Reliability modeling for dependent competing failure processes with changing degradation rate. *IIE transactions*, 2014, 46(5): 483-496.

[19] Becker G, Camarinopoulos L, Kabranis D. Dynamic reliability under random shocks. *Reliability Engineering & System Safety*, 2002, 77(3): 239-251.

[20] Ruiz-Castro J E. Markov counting and reward processes for analysing the performance of a complex system subject to random inspections. *Reliability Engineering & System Safety*, 2016, 145: 155-168.

[21] Peng W, Li Y F, Yang Y J, et al. Bayesian Degradation Analysis With Inverse Gaussian Process Models Under Time-Varying Degradation Rates. *IEEE Transactions on Reliability*, 2017, 66(1): 84-96.

[22] Zheng B, Li Y F, Huang H Z. Intelligent fault recognition strategy based on adaptive optimized multiple centers. *Mechanical Systems and Signal Processing*, 2018, 106: 526-536.

[23] Peng W, Balakrishnan N, Huang H Z. Reliability modelling and assessment of a heterogeneously repaired system with partially relevant recurrence data. *Applied Mathematical Modelling*, 2018, 59: 696-712.

[24] Guo J, Li Y F, Zheng B, Huang H Z. Bayesian degradation assessment of CNC machine tools considering unit non-homogeneity. *Journal of Mechanical Science and Technology*, 2018, 32(6): 2479-2485.

[25] Distefano S, Trivedi K S. Non‐Markovian State‐Space Models in Dependability Evaluation. *Quality and Reliability Engineering International*, 2013, 29(2): 225-239.

[26] Zio E, Pedroni N. Reliability estimation by advanced Monte Carlo simulation, Simulation Methods for Reliability and Availability of Complex Systems. Springer London, 2010: 3-39.

[27] Zio E, Librizzi M. Direct Monte Carlo Simulation for the Reliability Assessment of a Space Propulsion System Phased Mission. *Proceedings of the 8th International Conference on Probabilistic Safety Assessment & Management (PSAM)*. ASME Press, 2006.

[28] Mi J, Li Y F, Peng W, et al. Reliability analysis of complex multi-state system with common cause failure based on evidential networks. *Reliability Engineering & System Safety*, 2018, 174: 71-81.

[29] T. Khoda et al. Find Modules in fault trees. IEEE transactions on Reliability. Vol 38. No. 2, pp: 165-176, 1989.

[30] Li Y F, Mi J, Liu Y, et al. Dynamic fault tree analysis based on continuous-time Bayesian networks under fuzzy numbers. *Proceedings of the Institution of Mechanical Engineers, Part O: Journal of Risk and Reliability*, 2015, 229(6): 530-541.

[31] Huang H Z, Huang C G, Peng Z, et al. Fatigue Life Prediction of Fan Blade Using Nominal Stress Method and Cumulative Fatigue Damage Theory. *International Journal of Turbo & Jet-Engines*, 2017. DOI: https://doi.org/10.1515/tjj-2017-0015.

[32] Yang Y J, Peng W, Zhu S P, Huang H Z. A Bayesian approach for sealing reliability analysis considering the non-competing relationship of multiple degradation processes. *Ekcsploatacja i Niezawodnosc – Maintenance and Reliability*, 2016, 18(1): 10-15.

[33] Li X Y, Huang H Z, Li Y F. Reliability analysis of phased mission system with non-exponential and partially repairable components. *Reliability Engineering & System Safety*, 2018, 175: 119-127.

[34] Li X Y, Huang H Z, Li Y F, et al. Reliability assessment of multi-state phased mission system with non-repairable multi-state components. *Applied Mathematical Modelling*, 2018, 61: 181-199.